§22. Study of Transport Characteristics of Multiple Impurities Depending on the Impurity Source Location in LHD

Sudo, S., Tamura, N., Muto, S., Suzuki, C., Funaba, H., Murakami, I.

In magnetic confined plasmas, the accumulation of impurities (including helium ash) is one of concerned subjects. The impurity confinement time usually increases with the density in a helical system, while the high density operation is one of candidates for the helical type fusion reactor scheme. Considering this, we investigated the impurity behaviors in the plateau and PS regimes (based on the impurity – proton collision frequency) by injecting a tracer-encapsulated solid pellet (TESPEL)[1)] into a plasma of Large Helical Device (LHD). Kα intensities of the triple tracers, V (Z=23), Mn (Z=25) and Co (Z=27) in the two different collisional regimes[2)] are shown in Fig.1. Kα emissions come mainly from the plasma core. In the plateau regime (n_e= 3-4×10^{19} m^{-3}), they decay in ~0.5 s, while they are kept almost constant in the PS regime (n_e= 5-7×10^{19} m^{-3}). It should be noted that there are no significant differences in the temporal evolution for the different species of the tracers. The calculations with the assumed diffusivity D (spatially flat) and the inward pinch V (the peak value of -2 m/s at r_{eff}/a_{99}= 0.9) by one dimensional impurity transport code, STRAHL are also shown. In these cases, the tracer penetration depth is r_{eff}/a_{99}= ~0.75 or somewhat deeper. Thus, it is interested to see the behavior of the tracers in case of the shallower penetration. Recently we could achieve shallower deposition around r_{eff}/a_{99}= ~0.85 with a shell type TESPEL with a diameter of 0.6 mm and a thickness of ~75 μm. The tracers deposited in this location have still the same feature as the case of r_{eff}/a_{99}= ~0.75. So, the source location for having the impurity feature of long confinement in the PS regime is identified as at least up to r_{eff}/a_{99}= ~0.85.

For the further shallower deposition, we made a thin shell-type TESPEL consisting of $(C_8H_6Cl_2)_n$. In this case, Cl performs a role of tracer. Thus, more outer deposition locations of the tracers become possible. In fact, as shown in Fig. 2, the Li-like emissions from the Cl tracer stemming from the shell and the V tracer stemming from the central core of the TESPEL in the high density case are compared with the data calculated by the STRAHL code. The Cl Li-like emission observed experimentally decays faster than the calculated one compared to the case of the V Li-like emission. This indicates the existence of the shield effect of the impurity in the plasma periphery.

On the other hand, in order to see the behavior of the impurities coming from the outside of the plasma, we implemented a supersonic Ar gas puffing in addition to the TESPEL injection. In the medium density case, the Ar Kα emission was clearly observed together with the Kα emissions from the tracers. In contrast to this, the Ar Kα emission was drastically decreased in the high density case as shown in Fig. 3. This result shows the suppression of the intrinsic impurity coming from the outside of the plasma is indeed working in the high density case, while the impurities deposited inside the plasma is kept for a long time. In contrast to this, the Ar Li-like emissions mainly coming from the plasma periphery are observed in the both regimes[3)], which indicates the Ar penetration up to r_{eff}/a_{99}= ~0.9 in the high density case (or PS regime).

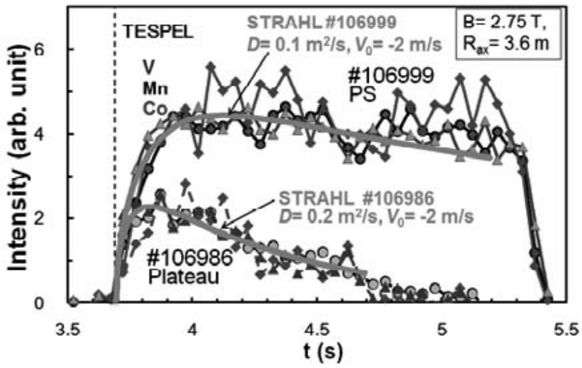

Fig.1 Temporal evolution of the Kα intensities from the tracers, V, Mn and Co in the two different collisional regimes. The calculated data by the STRAHL code are also shown.

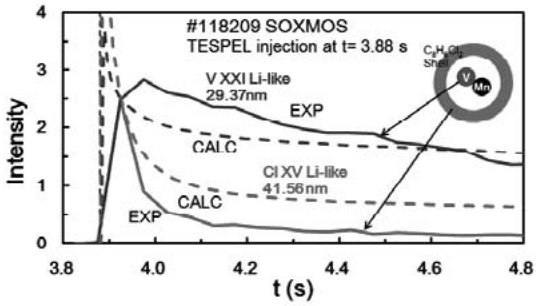

Fig. 2 Temporal evolution of the Li-like emission of the tracer V, and the Li-like emission of Cl contained in the thin-shell. The intensities calculated by the STRAHL code are also shown by the broken lines.

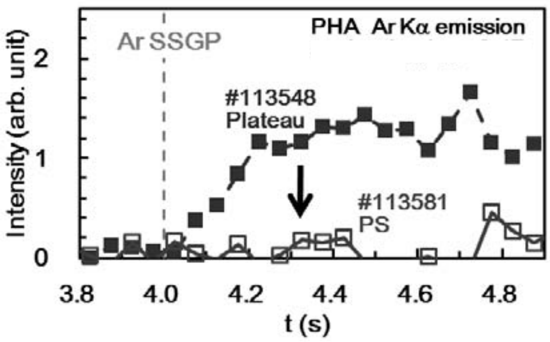

Fig.3 Kα emissions of gas puffed Ar in the two different collisional regimes.

1) Sudo, S. *et al. Rev. Sci. Instrum.* **83** (2012) 023503.
2) Sudo, S. *et al. Nucl. Fusion* **52** (2012) 063012.
3) Sudo, S. *et al Plasma Fusion Res.* **9** (2014) 1402039.